Physica 3D (1981) 605–617
North-Holland Publishing Company

ON DETERMINING THE DIMENSION OF CHAOTIC FLOWS

Harold FROEHLING, J.P. CRUTCHFIELD, Doyne FARMER, N.H. PACKARD and Rob SHAW
Physics Department, University of California, Santa Cruz, CA 95064, USA

Received 20 August 1980

We describe a method for determining the approximate fractal dimension of an attractor. Our technique fits linear subspaces of appropriate dimension to sets of points on the attractor. The deviation between points on the attractor and this local linear subspace is analyzed through standard multilinear regression techniques. We show how the local dimension of attractors underlying physical phenomena can be measured even when only a single time-varying quantity is available for analysis. These methods are applied to several dissipative dynamical systems.

1. Introduction

Recent progress in dynamical systems theory has strengthened the connection between "strange" or "chaotic" attractors and aperiodic behavior found in nature [1, 2, 3, 4]. Furthermore, Couette flow experiments performed near the transition from laminar to turbulent behavior suggest that fluid motion in the weakly turbulent regime can be understood in terms of low-dimensional chaotic attractors [5, 6]. Thus it is possible that weakly turbulent fluid flow, which in principle must be considered as an infinite-dimensional system, can be modeled by a system with relatively few phase-space dimensions. Many natural phenomena, in contrast to this, exhibit aperiodic behavior that can only be explained by a model with a very large number of dimensions. A model of thermal noise in a resistor, for instance, must account for the motions of the individual electrons within the resistor; the number of electrons involved is so large that any signal derived from the system appears "noisy". As a first step in modeling systems exhibiting aperiodic behavior, then, we must distinguish between those having an underlying low-dimensional chaotic attractor, and those requiring a large number of phase-space dimensions for a dynamical description.

Current techniques of data analysis, applied to aperiodic physical phenomena, cannot resolve these two fundamentally different sources of behavior. Power spectral analysis, for example, characterizes aperiodic behavior by the presence of broadband noise in the power spectrum, but broadband noise can be produced by systems requiring either a small or large number of phase-space dimensions. Thus the power spectrum fails to make this distinction. Low- and high-dimensional aperiodicity must instead be distinguished by a direct measurement of the number of coordinates needed to specify the state of the physical system under observation. Applied to fluid turbulence, this measurement might indicate that a chaotic attractor underlies weakly turbulent fluid flow. If a chaotic attractor exists for such flows, then the dimension would provide an experimental classification of turbulent flows.

We will describe a technique that measures the dimension of attractors in dissipative systems. More precisely, the technique measures the *approximate fractal dimension* by examining small regions of an attractor and determining whether or not the points of the attractor in each small region lie in or close to linear subspaces of dimension less than that of the phase space used to represent the system's states. From this perspective, the limit cycle attractor of the Van der Pol oscillator (a two-dimensional dynamical system) appears one dimensional, since lines (one-dimensional linear sub-spaces) are a suitable approximation to local regions of the attracting limit cycle. The simplest chaotic dynamical systems in three dimensions (such as those of Lorenz [1] and Rössler [7]) have attractors that appear locally two-dimensional. The method we introduce relies on standard multilinear regression techniques that measure the goodness of fit of linear subspaces to local regions of the attractor.

The application of this method requires an experimentalist to first develop a phase space representation of the dynamics under observation. Many experiments provide no clue at all as to which measured quantities might correspond to useful phase space coordinates. We will discuss these problems, and give examples for which unambiguous results can be obtained using phase space coordinates reconstructed from a single time series [8, 9].

2. Geometry of strange attractors

Since we are seeking a description of experimentally observable chaotic dynamics, we now review some geometrical and topological features of simple chaotic systems.

The phase space of a dissipative dynamical system can be divided into regions in which motion is unbounded and regions in which the motion is attracted into compact subsets. These compact subsets are called *attractors*, the set of all phase space points which asymptotically tend to an attractor is called its *basin of attraction.*

Certain asymptotic properties of a dynamical system's attractor are characterized by the attractor's spectrum of Lyapunov characteristic exponents (LCE's). There are as many characteristic exponents as there are dimensions in the phase space of the dynamical system. The LCE's measure the average rate of exponential convergence of trajectories onto the attractor when negative, and the average rate of exponential divergence of nearby trajectories within the attractor when positive. The magnitude of an attractor's positive exponents is a measure of its "degree of chaos" [10, 11].

The spectrum ot LCE's yields a useful classification of attractors. For example, in three dimensions a dynamical system with all negative exponents is a fixed point: the LCE spectrum is denoted by (−−−). A limit cycle attractor has an LCE spectrum of (0−−). A two-torus attractor has an LCE spectrum of (00−). Chaotic attractors in three dimensions have an LCE spectrum of (+0−). In this case the positive exponent indicates exponential spreading within the attractor in the direction transverse to the flow and the negative exponent indicates exponential contraction onto the attractor. Under the action of such a flow, phase space volumes evolve into sheets, as illustrated in fig. 1. For attractors in three dimensions then, the spectrum of characteristic exponents gives a rough measure of dimension. As a first step toward a dimensional classification of attractors, we can identify the dimension of an attractor with the number of non-negative characteristic exponents (we will make this notion more precise later): the (−−−) fixed point is zero-dimensional, the (0−−) limit cycle is one-dimensional, and the (00−) two-torus is two dimensional.

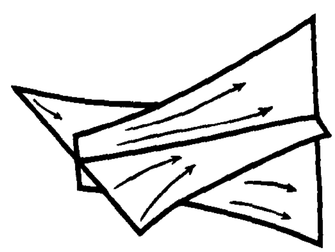

Fig. 1. Under the action of 3-dimensional flows with local exponential spreading transverse to the flow and exponential contraction in the other dimension, phase space volumes evolve into sheets.

The (+0−) chaotic attractor is also two dimensional, but its structure is actually more complicated than simple sheets: exponential divergence of nearby trajectories within a compact object requires the "folding" of sheets. A simple example of this process is illustrated in fig. 2. Trajectories diverge exponentially within a sheet; then the sheet folds and connects back to itself, forming an attractor which bears a striking resemblance to the attractor (shown in fig. 3) in a system due to Rössler [7],

$$\begin{aligned} \dot{x} &= -y - z, \\ \dot{y} &= x + ay, \\ \dot{z} &= b + xz - cz, \end{aligned} \tag{1}$$

with parameter values of $a = 0.2$, $b = 0.2$, and $c = 5.7$. The attractor is not simply a sheet with a single fold, but a sheet folded and refolded infinitely by the flow. A line segment which cuts the attractor transverse to these sheets will intersect the attractor in a Cantor set. The attractor has topological dimension two, but a fractal dimension [12] greater than two.

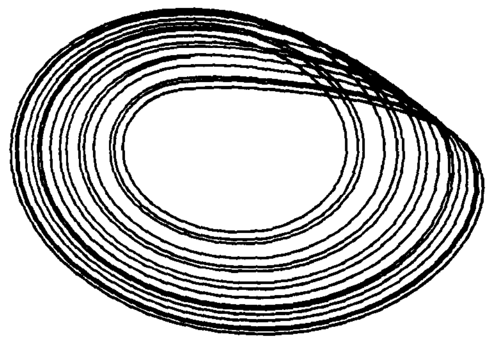

Fig. 3. X–y projection of Rössler attractor.

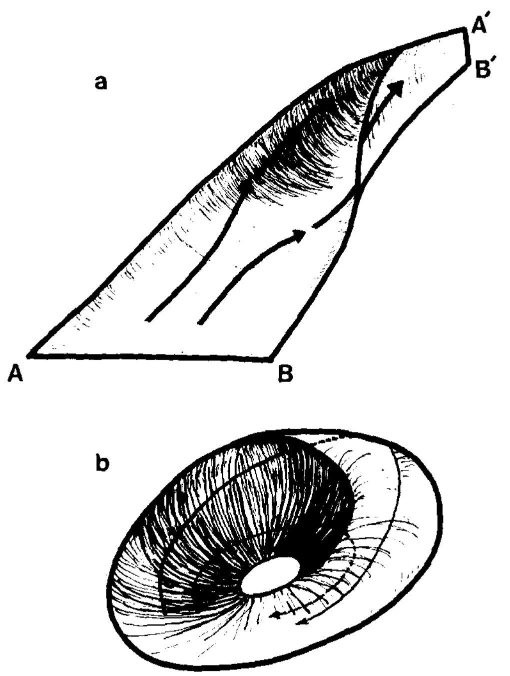

Fig. 2. (a) Exponential divergence of nearby trajectories within a compact object requires folding of sheets: connecting points A and A' together and B and B' together results in the object of (b).

To clarify the notion of fractal dimension, imagine a box which contains a small region of an attractor. If this box is subdivided into smaller boxes, some fraction of the smaller boxes will contain pieces of the attractor, while the rest won't. For example, if the small region of the attractor is a simple plane, and if a 3-dimensional box which contains it is divided by 10 in each dimension (for a total of 1000 smaller boxes), then roughly 100 of these smaller boxes will contain pieces of the plane. The number of piece-containing boxes will scale as L^d, where L is the factor by which each dimension of the box is divided. This construction defines the fractal dimension [13]:

$$d = \lim_{\epsilon \to 0} \frac{\log N(\epsilon)}{\log(1/\epsilon)}, \tag{2}$$

where $N(\epsilon)$ is the number of boxes, whose sides have length ϵ, necessary to cover the attractor. For a plane d is 2 by this construction, the same as the topological dimension. The simplest chaotic attractors (those lying in a 3-dimensional phase space) have fractal dimension between 2 and 3; d then measures how "closely packed" the sheets of an attractor are.

Mori [14] conjectured one relationship between an attractor's fractal dimension and its spectrum of Lyapunov exponents, but numerical evidence [15] supports a conjecture by Kaplan and Yorke [16],

$$d = j + \frac{\sum_{i=1}^{j} \lambda_i}{-\lambda_{j+1}}, \tag{3}$$

where we assume the Lyapunov exponents to be ordered, $\lambda_1 > \lambda_2 > \ldots . > \lambda_N$, and where j is the largest integer so that $\lambda_1 + \cdots + \lambda_j > 0$. The Rössler attractor, with parameter values $a = 0.2$, $b = 0.2$, $c = 5.7$, has an LCE spectrum of (0.075, 0, −5.372) [17]. According to eq. (3) then, this attractor has a fractal dimension of 2.014.

In discussing global properties, Williams [19] and Shaw [20] "collapse" the fractal structure to simple folded sheets by taking a neighborhood of the attractor and identifying all points within the neighborhood that become arbitrarily close under the action of the flow. They call the resulting object the attractor's "branched manifold". Any experiment, either physical or numerical, through its finite resolution automatically makes this identification: at any degree of resolution an observer sees only a branched manifold.

3. Phase space reconstruction

Certain experimental systems can be modeled by systems of ordinary differential equations. Stirred chemical reactions [9] are an example: the concentrations of various compounds and intermediates serve as coordinates in phase space. In these cases one can make an unambiguous identification between the available experimental quantities and the phase space coordinates of our dynamical systems approach. With these coordinates, determination of the attractor's dimension should be straightforward.

An experimental system modeled by partial differential equations presents greater difficulties. To obtain a complete dynamical description of a fluid its velocity at every point must, in principle, be known. But to determine the dimension of a low-dimensional attractor only a few independent quantities are needed: as few as the fractal dimension of the attractor rounded to the next high integer. Even if a low-dimensional attractor underlies fluid flow, the experimentally accessible quantities which contain the information necessary to reconstruct a phase space picture of the dynamics are not given a priori. The notion of obtaining a picture of a system's dynamics by viewing attractors projected onto a space of experimentally accessible quantities was first introduced by R. Abraham [21], who called these projections "macrons".

The problem of reconstructing a finite-dimensional phase space picture that gives a faithful representation of fluid motion (after transients have died away) is not yet settled. Packard et al. [8] mention as possibilities time derivatives, time delays [22], and even spatially separated sampling. J.C. Roux et al. [9] reconstructed a chaotic attractor from chemical turbulence using one time-varying signal and its derivatives. Although in the following sections we use time delays as an example of a reconstruction technique, the experimentalist must take our suggestions as tentative, not final. The relative merits of different techniques must be carefully considered for each new experimental situation.

In reconstructing a phase space it is necessary that the fractal dimension of the attractor lying in the original and reconstructed phase spaces be the same. For systems of ordinary differential equations the meaning of "original phase space" is clear. For a physical system the original phase space is the space of all possible initial conditions, which in general will have a much larger dimension (possibly infinite) than that of the attractor describing the asymptotic state of the system.

A simple and adequate technique for reconstructing an N-dimensional phase space, from a single time series with time delay Δt between samples, equates the reconstructed phase space point with N successive points of the time series separated by a delay $n\Delta t$. The next phase space point is found by advancing each previous point by a time Δt. Unfortunate choices for N, n, or Δt may grossly distort the phase space portrait of the original attractor: although the dimension may not change, it may for practical purposes become nearly impossible to measure.

Fig. 4 shows the Rössler attractor reconstructed from a single time series using this method. There is an obvious similarity between this attractor and the original attractor shown in fig. 3. In section 5 we show that the two attractors have the same approximate fractal dimension. As an example of an unfortunate choice of variables, the reconstructed Rössler attractor would be unrecognizable if the time delay Δt were simply rationally related to the average period of this system.

This technique reconstructs an object in an N-dimensional phase space from a single time series. But in experimental situations N need not equal the dimension of the phase space of the phenomenon studied. In the next section we will show that, as long as N is chosen greater than the dimension of the attractor in the original phase space, the attractor's approximate fractal dimension can be determined unambiguously.

4. Local determination of the approximate fractal dimension

The concept of dimension evolved slowly from the turn of the century when Poincare set out its basic definitions [23]. Practical application of these notions, however, flourished only with the advent of modern computers, which allowed for the development of techniques for dimension measurement. Questions about the dimension associated with a given data set were first addressed by Shepard in 1962 [24] to measure the number of significant parameters in psychological experiments. Since then, techniques have been refined to measure

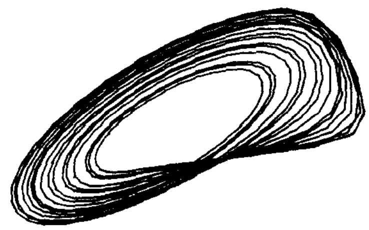

Fig. 4. X–y projections of Rössler attractor reconstructed from a time series: $\Delta t = 0.2$, $N = 3$, $n = 1$. This reconstructed attractor fits in a three dimensional box roughly 20 units on a side.

the "intrinsic" dimension of data [25] in a wide range of fields including signal analysis [26] and pattern recognition [27]. We shall now extend some ideas related to this earlier line of inquiry to the context of dynamical behavior.

Packard et al. [8] discuss several techniques that measure the approximate fractal dimension of attractors. Takens [28] has also recently proposed a technique for measuring the fractal dimension as well as the topological entropy of an attractor. Unfortunately, these methods appear to be sensitive to instrumental noise, and they require an unduly large number of data points. In what follows we present a practical algorithm which is substantially less sensitive to noise.

After collecting N-dimensional phase space points that presumably lie on an attractor with approximate fractal dimension N-1 or less, we require for the following discussion that the phase space be partitioned so that each portion of the imbedded attractor is approximately flat. This partition is accomplished by sorting the phase space data into N-dimensional "boxes" according to their coordinate value in each dimension. If the phase space points in each box lie close to a piece of a manifold or branched manifold we can describe these points as lying approximately in a linear space of dimension less than N. Multilinear regression is the natural analysis to apply to these points: on N-dimensional phase space point it finds the best hyperplane (dimension N-1 or less) that fits the data. By using smaller dimensional phase spaces we can fit smaller-dimensional linear subspaces. The goodness of fit in each box is measured by χ^2, the sum of the squares of the deviations from this hyperplane divided by the number of degrees of freedom.

If the dimension of the hyperplane is too small the fit will typically be poor and χ^2 will be large. When the dimension is increased so that the hyperplane gives a good fit to the data, χ^2 will drop sharply. The dimension of this hyperplane provides the closest integer approximation to the fractal dimension, which we call the *approximate fractal dimension.*

We display the results of this Local Linear Regression (LLR) in a histogram of the logarithm of χ^2, showing the number of occurrences of ranges of χ^2 for regions of the attractor where the analysis is applicable. In the following histograms five columns represent a factor of ten difference in χ^2; every tick mark on the vertical axis represents ten occurrences of a particular range of χ^2.

Figure 5 shows the χ^2 histograms for Rössler attractor. The greatest number of occurrences of χ^2 for planes occurs lower by a factor of one million than the peak in occurrences for points and lines, indicating that the Rössler attractor looks locally planar. That some local regions have poor plane fits is due to the branched manifold structure mentioned above.

There is another quantity arising in LLR which also characterizes the dimension of an attractor. If too many phase space coordinates are chosen the system of equations determining the hyperplane is overdetermined: the resulting correlation matrix will be singular. (With noise in the system the correlation matrix will be approximately singular.) This fact can be used to determine the number of independent quantities needed to specify a physical system, although we will not develop this approach here.

χ^2 of multilinear regression measures the deviation of the "dependent variable" from the best fit hyperplane, not the perpendicular deviation of the points from a hyperplane. Thus χ^2 would be measured as overly large if one or more slopes were appreciable, and the χ^2 histogram would not accurately reflect the actual deviations from a hyperplane. As a practical remedy we perform multilinear regression twice for each local region. The first calculation of best fit hyperplane is used to rotate the points in the local region so that all slopes are zero; then for the second multilinear regression the deviation of the dependent variable from a hyperplane is approximately the true perpendicular deviation.

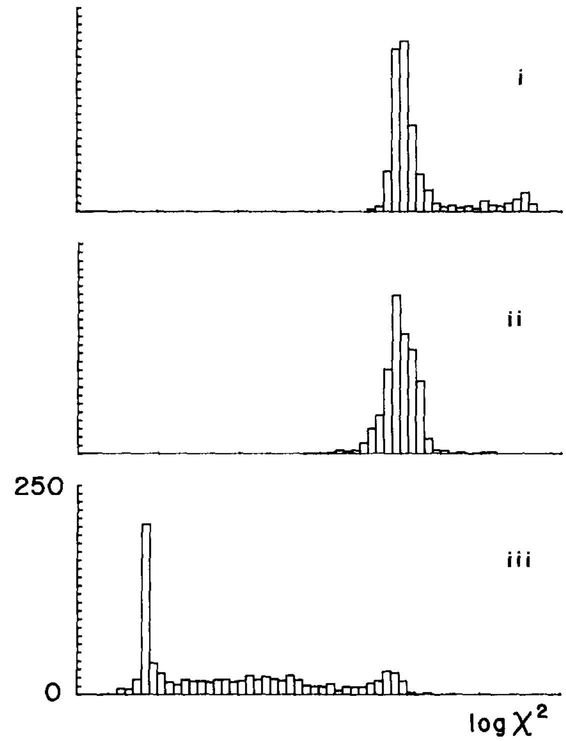

Fig. 5. Chi-squared histograms for Rössler attractor using natural coordinates, $\Delta t = 0.2$, box size = 0.5, noise $\sigma = 0.01$ (= 0.1%) added, 10,000 3-D points: (i)–(iii) best fit points, lines, and planes. On this and all succeeding histograms, every five columns on the horizontal axis represent a factor of 10 difference in χ^2; every tick mark on the vertical axis represents 10 occurrences of a particular range of χ^2.

5. Choosing a delay time

We have given evidence that the system of phase space coordinates reconstructed from a time series can be a suitable replacement for the original (possibly unknown) system. The time interval between successive samples in a time series is as yet undetermined. For the state space construction from a time series to be of practical use, we must either specify a way to choose an optimum time interval, or show that the results are relatively insensitive to the time interval chosen. Systems with chaotic attractors offer an upper limit to this time interval, corresponding roughly to the average time between "folding" of adjacent sheets of the attractor. If trajectories from different sheets approach one another exponentially, then in some finite time they will for all practical purposes become identified; a bit of information is lost, corresponding to which sheets the trajectories were on. Thus if we choose too long a time interval we can no longer make a one-to-one correspondence with points of the time series and the original attractor. For attractors that are not chaotic (solutions lying on an n-torus, for instance) there is no upper limit on the time interval. In our numerical studies we typically chose the delay time to be approximately 10% of the folding time.

A qualitative lower limit also exists. If the time interval is chosen too small, then the N successive points are all approximately equal; the attractor appears "stretched out" along the $x = y = z = \ldots$ direction. This problem with short time intervals could be alleviated by taking appropriate differences between coordinates and dividing by the time interval (analogous to taking derivatives), but this procedure introduces noise into the phase space picture. Choosing $n\Delta t$ of our reconstruction technique sufficiently large obviates the need for this noise-producing procedure.

Our experience indicates that any time interval between these extremes is a suitable one. Of course, if the system is periodic or quasiperiodic and one chooses a time interval simply rationally related to a period, the results will be misleading.

As a check on the relative insensitivity of results with time interval (within extremes), we have performed LLR on the Rössler attractor reconstructed from a time series by the method in section 3. Fig. 6 shows the histograms for the Rössler attractor for time increments of 0.1, and delays of 5, 10, and 20 time increments between coordinates. The results show that for each time interval, a local 2-dimensional surface (plane) fits the data much better than lines or points.

Fig. 6 also illustrates the effect of choosing too many coordinates to describe a system. A four-dimensional phase space was reconstructed from the time series using delays, although only three independent quantities are needed to describe points on the attractor. The correlation matrices needed to calculate χ^2 are approximately singular when trying to fit 3-D linear subspaces to 4-D points; still, the χ^2 histograms for these indicate fits as good as those for planes. Normally one would check the values of the correlation matrix to avoid any possible problems.

Notice that the time interval we recommend is of the same order as typical sampling times used in power spectral analysis. In fact, the same time series used for power spectral analysis may be used for LLR with absolutely no change.

6. Noise and curvature

The technique of LLR naturally accommodates deviation from a hyperplane. But two sources (excluding branched manifold structure) contribute to this deviation: (1) observational noise in the data and (2) curvature of the attractor.

It is possible to distinguish these two sources of deviation. If the box size is decreased the deviation from a hyperplane will decrease, since the deviation due to curvature is decreased. As the box size decreases, eventually observational noise becomes the only source of deviation.

The ability to measure the dimension of an

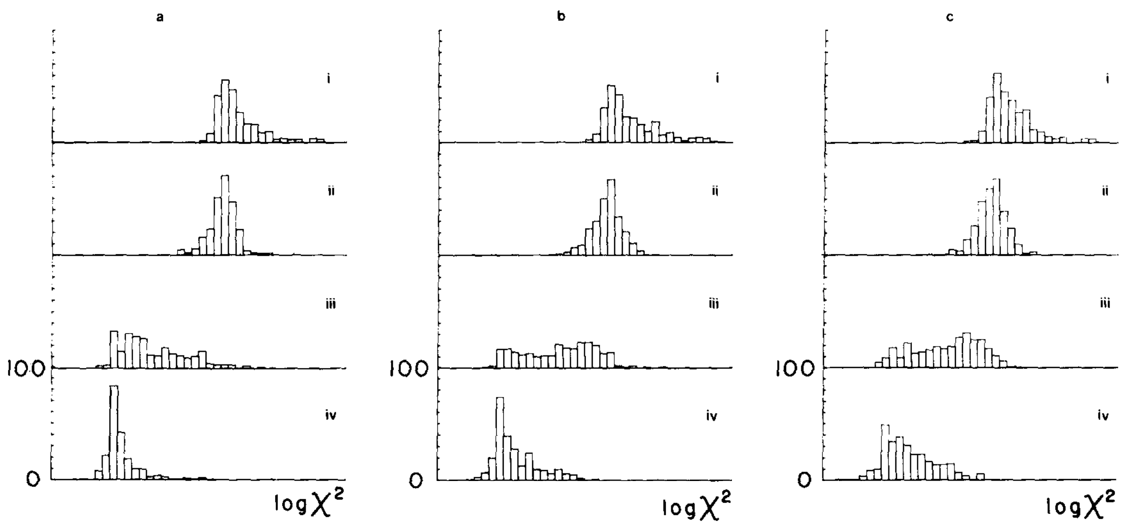

Fig. 6. Chi-squared histograms for Rössler attractor reconstructed from a time series, $\Delta t = 0.2$, box size = 1.0, 10,000 4-D points, noise $\sigma = 0.01$ (= 0.1%) added: (a) delay = 5 time intervals: (i)–(iv) best fit subspaces of 0, 1, 2, and 3 dimensions; (b) delay = 10 time intervals: (i)–(iv) best fit subspaces of 0, 1, 2, and 3 dimensions; (c) delay = 20 time intervals: (i)–(iv) best fit subspaces of 0, 1, 2 and 3 dimensions.

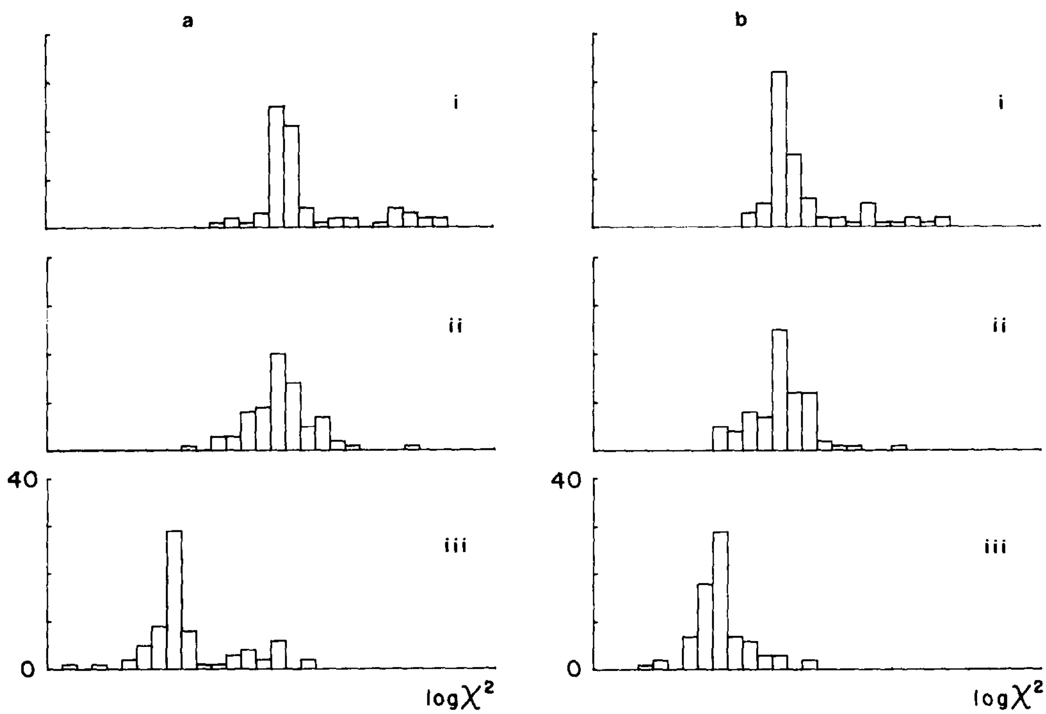

Fig. 7. Chi-squared histograms of Rössler attractor reconstructed from a time series, $\Delta t = 0.2$, time delay = 5 box size 2.0, 5,000 points: (a) noise $\sigma = 0.1$ (= 1%) added: (i)–(iii) best fit points, lines, and planes; (b) noise $\sigma = 0.2$ (= 2%) added: (i)–(iii) best fit points, lines, and planes.

attractor in the presence of noise depends on both the magnitude of the noise compared to the size of the attractor, and the box size. To reliably detect a hyperplane the size of the box must be larger than the noise. But if the noise is too large we must choose a box whose size is of the same order of magnitude as (or larger than) the curvature of the attractor and any attempt to fit a hyperplane must result in a large χ^2; the hyperplane fit fails.

By this method the dimension of chaotic attractors can be reliably measured even when observation noise is appreciable, if the geometry of these attractors is simple. Fig. 7 shows χ^2 histograms for the Rössler attractor, with zero-mean Gaussian random noise of standard deviations 0.1 and 0.2 added to the signals. These correspond roughly to 1% and 2% noise relative to the size of the attractor. In both cases planes fit the data significantly better than points or lines. For noise levels much greater than this a determination of the dimension becomes difficult.

7. The effect of fractal structure

The Rössler attractor shown in fig. 3 has strong contraction of phase space volumes effectively truncating its fractal structure to a branched manifold after a small fraction of a revolution around the attractor. To examine the effect of fractal structure on determining the dimensionality of chaotic attractors we have studied the scaling properties of the Hénon map [29] which has weak convergence of adjacent folds of the attractor.

$$x_{i+1} = y_i + 1 - ax_i$$
$$y_{i+1} = bx_i. \tag{4}$$

This 2-dimensional system clearly reveals many leaves of the fractal structure. Fig. 8 shows the Hénon map and χ^2 histograms for the Hénon map. The histograms are qualitatively the same for the different box sizes, showing that even for substantial fractal structure we can confidently determine the approximate fractal dimension of an attractor.

8. Direct calculation of the fractal dimension

The sorting necessary to use LLR offers the information necessary to estimate the fractal dimension using the scaling construction of eq. (2). For 20,000 2-dimensional points we measure

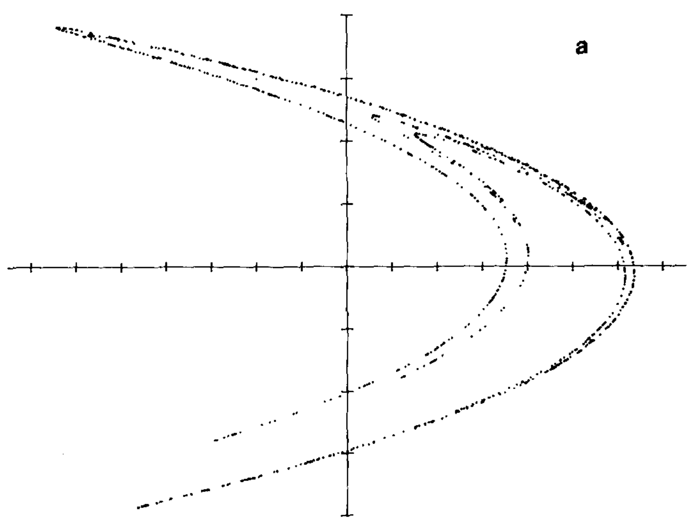

Fig. 8(a)

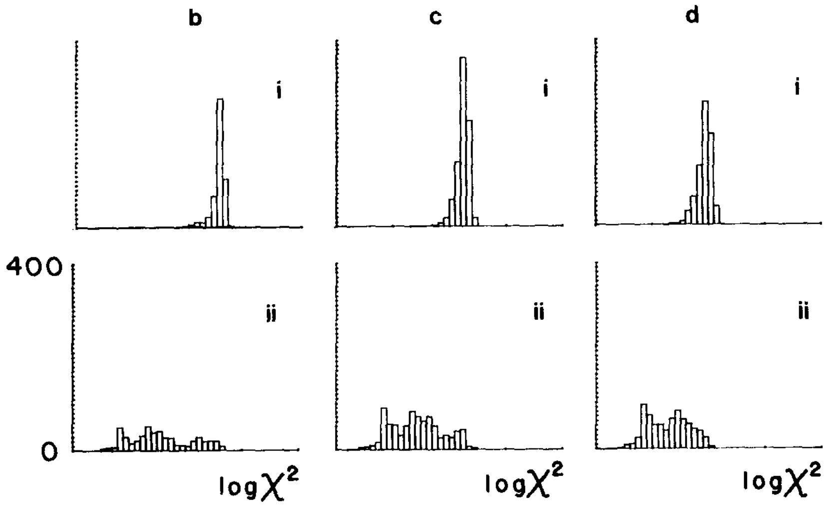

Fig. 8. (a) Hénon map, $a = 1.4$, $b = 0.3$, 1000 2-D points, noise $\sigma = 0.0001$ (= .01%) added (b) box size = 0.005: (i)–(ii) best fit points and lines (c) box size = 0.01: (i)–(ii) best fit points and lines; (d) box size = 0.02: (i)–(ii) best fit points and lines

a fractal dimension

$$d = 1.19,$$

while eq. (3) gives a fractal dimension of

$$d = 1.26,$$

and Simó [30] finds

$$d = 1.2365.$$

Since we define the surface of the attractor by the points lying on it, we expect our scaling construction to underestimate the fractal dimension because as we take smaller boxes, some will not contain any points, simply because they have not yet been visited, although pieces of the attractor lie within them. Unfortunately, this simple estimate of the fractal dimension becomes even more inaccurate for higher-dimensional attractors, and its use appears impractical for even sheet-like structures for this reason.

9. Data acquisition requirements

In principle, the LLR technique will work for attractors of any dimension. Unfortunately, there are practical limitations that prevent this from being feasible for attractors of dimension greater than about five. These limitations are also present, and in fact they are more severe, for the straightforward determination of the fractal dimension as outlined in section 8.

In order to fit an m-dimensional hyperplane, at least $m + 1$ points are required. Thus for a given box it is necessary to collect points from the time series until at least $m + 1$ points have been found that lie inside the box. The length of the time series that is needed to do this may be estimated by assuming that the points of the sampled time series are uniformly distributed over the attractor. Using D-dimensional boxes of diameter ϵ, the number of boxes required to cover the attractor is $N(R) \approx R^D$, where $R = 1/\epsilon$ is the resolution used in constructing the cover of boxes. The probability of finding a point in any box is roughly $1/N$, so the number of points that must be examined to make it likely to find a single point in any given box is $\approx N$. For a successful determination of the dimension of the best fit hyperplane for the points in a box, at least $D+1$ points are needed. The number of data points n that must be taken is therefore

$$n \approx (D+1)N \approx (D+1)R^D.$$

For reasonable values of R, this number becomes very large when D exceeds 5. For example, if $R=20$ and $D=5$, $n \approx 2\times 10^7$. For typical rates of data acquisition, it is often impractical to gather or process this many data points.

For LLR the situation is improved slightly because it is not necessary to gather sufficient points in every box, but rather only to gather points in enough boxes to gain a representative sample of boxes covering the attractor. Since the points on an attractor do not typically have uniform distribution, the more probable boxes will fill out much earlier than others, reducing the number of data points that must be examined.

A nonuniform distribution of points works *against* a direct measurement of the fractal dimension based on eq. (2), such as that made for the Hénon map in section 8. To measure the fractal dimension directly from the definition it is necessary to count the number of boxes required to cover the attractor at several levels of resolution. For a uniform distribution, this typically takes considerably more than $n = R^D$ points; if the distribution is uneven, this problem becomes worse. In addition, for a direct determination, sufficient computer memory must be allocated to cover the attractor. For many applications this proves to be a more severe constraint than does the problem of gathering and processing sufficient data.

In summary, we have shown that this technique may be feasibly applied to physical systems that are described by low dimensional attractors. Thus, this may be useful for studying fluid flows such as those found near the transition to turbulence. For fully developed turbulence this technique, or any technique that requires sufficient data points to cover the attractor with moderate resolution, will certainly be impractical.

10. Other systems

Fig. 9 shows the results of LLR for x–y–z coordinates of the Lorentz system [1]

$$\begin{aligned} \dot{x} &= -10x + 10y, \\ \dot{y} &= -xz + 28x - y, \\ \dot{z} &= xy - (8/3)z. \end{aligned} \tag{5}$$

We interpret the results as indicating that local 2-D surfaces are almost everywhere good fits; not all plane fits are good, indicating the branched manifold structure of the attractor.

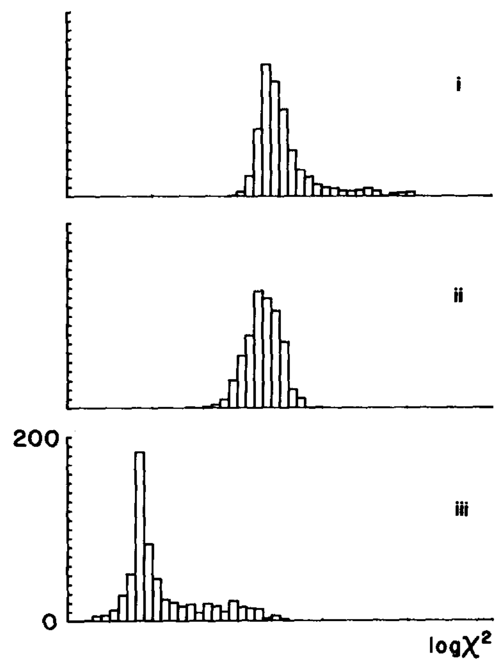

Fig. 9. Chi-squared histograms for Lorentz system, $\Delta t = 0.2$, time delay = 5, box size = 1.0, noise $\sigma = 0.01$ (= 0.1%) added, 10,000 3-D points: (i)–(iii) best fit points, lines, and planes.

It is difficult for LLR to distinguish between LCE signatures of (+0−), a branched manifold attractor, and (00−), a torus. However, LLR analysis, in conjunction with power spectral analysis, does distinguish these two very different types of attractor. A power spectrum of a 2-torus has sharp peaks corresponding to two incommensurate frequencies (along with harmonics and sums and differences of frequencies) but no broadband noise, while a chaotic system is characterized by broadband noise in its power spectrum. Thus we see that power spectral analysis and LLR give complementary information.

For 4-D systems LLR apparently cannot distinguish–even with power spectral analysis–between a (++0−) system and a (+00−) system: both will exhibit branched manifold structure and have broadband noise in their power spectra. An example of a (++0−) system is the Hyperchaos system of Rössler [31]:

$$\begin{aligned} \dot{x} &= -y - z, \\ \dot{y} &= x + 0.25y + w, \\ \dot{z} &= 3 + xz, \\ \dot{w} &= -0.5z + 0.05w. \end{aligned} \tag{6}$$

Fig. 10 shows the χ^2 histograms for this system. Locally 3-dimensional subspaces are better fits than points, lines, or planes. This agrees quite well with the fractal dimension $d = 3.006$ computed with eq. (3) from the characteristic exponent spectrum (0.121, 0.021, 0.005, −23.7) [17].

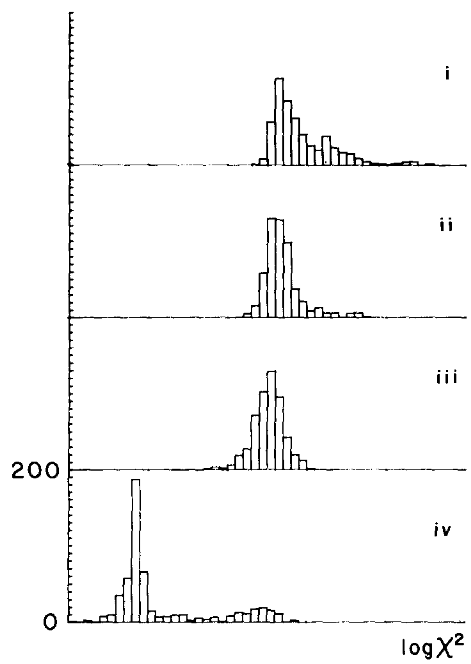

Fig. 10. Chi-squared histograms for hyperchaos system reconstructed from a time series, $\Delta t = 0.2$, time delay = 5, box size = 2.0, noise $\sigma = 0.01$ (= 0.1%) added, 20,000 4-D points: (i)–(iv) best fit local subspaces of 0, 1, 2, and 3 dimensions.

11. Conclusions

The method of multilinear analysis on neighboring points in phase space determines the dimension of an attractor. Phase space points may be chosen from successive points in the time series of some variable in a physical system when no a priori choice is clear. The dimension of simple attractors we have studied (as measured by a histogram of the logarithm of χ^2) is independent of this choice of phase space points; it is also relatively independent of the choice of time interval between successive points in a time series, and of the definition of propinquity of phase space points (size of box chosen).

The information obtained in performing local linear regression may also give quantitative information concerning the fractal nature of strange attractors. Furthermore, we hope to extend the method of LLR to calculate directly the Lyapunov characteristic exponents–either from known phase space coordinates or from a time series–in order to provide a classification of dynamical behavior found in physical systems. In light of these results LLR analysis may prove useful in fluid, chemical, and solid state turbulence experiments and in the understanding of other chaotic phenomena for which power spectral analysis proves inadequate to characterize a system's behavior.

Acknowledgements

DF would like to thank the Hertz Foundation for their support; JC NP, and RS gratefully acknowledge NSF support.

References

[1] E.N. Lorentz and J. Atmos. Sci. **20** (1963) 130.
[2] D. Ruelle and F. Takens, Comm. Math. Phys. **50** (1976) 69.
[3] B.A. Huberman and J.P. Crutchfield, Phys. Rev. Lett. **43** (1979) 1743.
[4] B.A. Huberman, J.P. Crutchfield and N.H. Packard, Appl. Phys. Lett. **37** (1980) 750.
[5] J. Gollub and H. Swinney, Phys. Rev. Lett. **35** (1975) 927.
[6] R.W. Walden and R.J. Donnelly, Phys. Rev. Lett. **42** (1979) 301.
[7] O.E. Rössler, Phys. Lett. **57A** (1976) 196.
[8] N.H. Packard, J.P. Crutchfield, J.D. Farmer and R.S. Shaw Phys. Rev. Lett. **45** (1980) 712.
[9] J.C. Roux, A. Rossi, S. Bachelart and C. Vidal, Phys. Lett. **77A** (1980) 391.
[10] I. Shimada and T. Nagashima, Prog. Theor. Phys. **61** (1979) 1605.
[11] G. Bennetin, L. Galgani and J.M. Strelcyn, Phys. Rev. **A14** (1976) 2338.
[12] B.B. Mandelbrot, Fractals: Form, Chance, and Dimension W.H. Freeman, San Francisco, (1977).
[13] Eq. (2) defines a set's *capacity*, which we will take to be the same as the Haussdorf–Besicovitch dimension for the attractors we study.
[14] H. Mori, Prog. Theor. Phys. **63** (1980) 1044.
[15] J.D. Farmer, N.H. Packard, Chaotic Attractors in Infinite-Dimensional Systems I: Differential Delay Equations, UCSC preprint, submitted to Physica D (1980).
[16] J. Kaplan and J. Yorke, Chaotic Behavior of Multidimensional Difference Equations, Springer Lecture Notes in Mathematics **730** (1979) 204.
[17] J.P. Crutchfield, Senior Thesis, University of California at Santa Cruz (1979).
[18] J.D. Farmer, J.P. Crutchfield, H. Froehling, N.H. Packard and R.S. Shaw, Annals, N.Y. Acad. Sci. **357** (1980) 453.
[19] R.F. Williams, Berkeley Turbulence Seminar, 1976–77, P. Benard, and T. Ratiu, eds., Springer Lecture Notes in Mathematics **615** (1977).
[20] R. Shaw, Z. Naturforsch. 36a (1981) 80.
[21] R. Abraham, in Evolution and Consciousness E. Jantsch and C.H. Waddington, eds., (Addison Wesley, Reading, Mass., 1976).
[22] D. Ruelle, private communication.
[23] H. Poincaré, The Foundations of Science (Science, Garrison, N.Y. 1913).
[24] R.N. Shepard, Psychometrika **27** (1962) 125; **27** (1962) 219.
[25] K. Fukunaga and D.R. Olsen, IEEE Trans. Comp. **C-20** (1971) 176.
[26] G.V. Trunk, IEEE Trans. Comp. **C-25** (1976) 165.
[27] L.J. White and A.A. Ksienski, Pattern Recognition **6** (1974) 35.
[28] F. Takens, Detecting Strange Attractors in Turbulence, preprint (1980).
[29] M. Hénon, Comm. Math. Phys. **50** (1976) 69.
[30] C. Simó, On the Hénon–Pomeau Attractor, preprint (1979).
[31] O.E. Rössler Phys. Lett. **71A** (1979) 155.